




Superconductivity in TlBi_2 with a large Kadowaki-Woods ratio


Zhihua Yang, Zhen Yang, Qiping Su , Enda Fang, Jinhu Yang, Bin Chen , and Hangdong Wang ^{*}
Hangzhou Key Laboratory of Quantum Matter, School of Physics, Hangzhou Normal University, Hangzhou 311121, China

Jianhua Du

Department of Physics, China Jiliang University, Hangzhou 310018, China

Chunxiang Wu

Department of Physics, Zhejiang University, Hangzhou 310027, China

Minghu Fang [†]

Department of Physics, Zhejiang University, Hangzhou 310027, China
and Collaborative Innovation Center of Advanced Microstructures, Nanjing University, Nanjing 210093, China



(Received 11 April 2022; revised 6 November 2022; accepted 15 November 2022; published 1 December 2022)

In this paper, the superconducting and normal state properties of TlBi_2 with the AlB_2 -type structure were studied by resistivity, magnetization, and specific heat measurements. It was found that bulk superconductivity with $T_c = 6.2$ K emerges in TlBi_2 , which is a phonon-mediated s -wave superconductor with a strong electron-phonon coupling ($\lambda_{ep} = 1.38$) and a large superconducting gap ($\Delta_0/k_B T_c = 2.25$). We found that the $\rho(T)$ exhibits an unusual T -linear dependence above 50 K, and can be well described by the Fermi-liquid theory below 20 K. Interestingly, its Kadowaki-Woods ratio A/γ^2 [$9.2 \times 10^{-5} \mu\Omega \text{ cm}(\text{mol K}^2/\text{mJ})^2$] is unexpectedly one order of magnitude larger than that obtained in many heavy fermion compounds, although the electronic correlation is not so strong.

DOI: [10.1103/PhysRevB.106.224501](https://doi.org/10.1103/PhysRevB.106.224501)

I. INTRODUCTION

MgB_2 , as a simple binary compound, has a rather high superconducting transition temperature ($T_c = 39$ K) compared with other conventional superconductors [1,2]. The first-principles calculations and the inelastic neutron scattering measurements revealed that the E_{2g} in-plane boron phonons near the Brillouin zone center strongly coupled to the planar boron σ bands [3,4], which leads to the high T_c in MgB_2 . Moreover, MgB_2 has the multiple bands with a weak electronic correlation [5–7], and the distinct multiple superconducting energy gaps [8,9], resulting in markedly novel behaviors in its superconducting and normal-state properties [2]. Although MgB_2 has been extensively studied, new physical phenomena are constantly discovered [10,11], so those superconductors with the same structure are worth revisiting.

The binary bismuthide TlBi_2 [12] crystallizes in a hexagonal AlB_2 -type structure, the same as MgB_2 , consisting of honeycombed bismuth layers and thallium layers located in between them, as shown in the inset of Fig. 1. Compared with MgB_2 , TlBi_2 contains the heavier elements, suppressing the high frequency lattice vibration, and being unfavorable to the high T_c superconductivity in the conventional electron-phonon coupling mechanism. Although

TlBi_2 was classified as a strong coupling superconductor with $T_c = 6.4$ K by Dynes in 1972 [13], its detailed physical properties are rarely investigated as compared with that of MgB_2 .

In this paper, we synthesized successfully the single phase polycrystalline TlBi_2 sample. The superconducting and normal-state properties were systematically studied by resistivity, magnetization, Hall resistivity, and specific heat measurements. We reconfirmed that type-II superconductivity with $T_c = 6.2$ K, the upper critical field $\mu_0 H_{c2} = 1.4$ T, and the lower critical field $\mu_0 H_{c1} = 1.08 \times 10^{-2}$ T emerge in the TlBi_2 compound. It was found that the electronic specific heat in the superconducting state can be well described using a single gap model within the Bardeen-Cooper-Schrieffer (BCS) framework. The strong electron-phonon coupling occurs in this compound, confirmed by both the large $\lambda_{ep} (= 1.38)$ and the large $\Delta_0/k_B T_c (= 2.25)$ values, indicating that TlBi_2 is a conventional superconductor. It was found that the temperature dependence of resistivity in the normal state, $\rho(T)$, exhibits an unusual linear behavior above 50 K, which is ascribed to the low-energy phonon scattering, while $\rho(T)$ below 20 K is well described by the Fermi liquid theory, i.e., $\rho(T) = \rho_0 + AT^2$. Combining the specific heat data at normal state, we found that its Kadowaki-Woods ratio (KWR), A/γ^2 [$9.2 \times 10^{-5} \mu\Omega \text{ cm}(\text{mol K}^2/\text{mJ})^2$], is unexpectedly one order of magnitude larger than that obtained in many heavy fermion compounds, although the electronic correlation is not so strong.

^{*}hdwang@hznu.edu.cn

[†]mhfang@zju.edu.cn

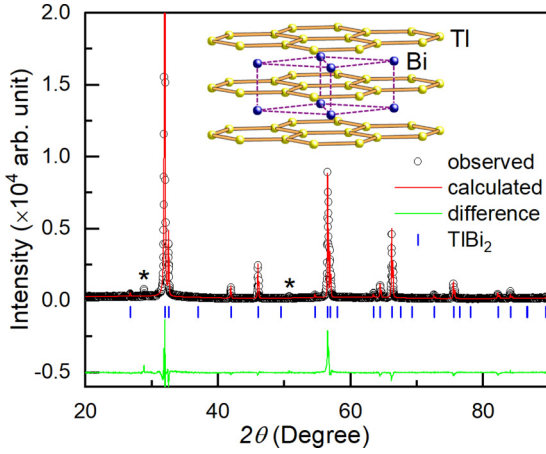


FIG. 1. Rietveld refinement profile of the polycrystalline XRD of TlBi_2 using the software RIETAN-2000 [15]. The resultant weighted reliable factor R_{wp} is 8.95%. Inset: The crystal structure of TlBi_2 . Thallium and bismuth atoms are drawn as dark-blue and yellow spheres, respectively.

II. EXPERIMENTAL METHODS

TlBi_2 polycrystalline samples were synthesized using the method as described before [14]. First, Tl and Bi lumps were

mixed and sealed in a vacuum quartz tube. Then, the mixture was melted over a flame and mixed carefully by shaking vigorously for 10 min. After that, TlBi_2 samples were annealed at 210°C for 2 wk. Last, the quartz tube was quenched into cold water to prevent the formation of impurity phases during the cooling process. In order to compensate for the loss of Tl due to the presence of Tl_2O_3 in the raw material, an additional 10% Tl was added. The obtained sample was easy to press into a flake and then cut into rectangular bars for later study. Polycrystalline x-ray diffraction (XRD) was performed on a Rigaku x-ray diffractometer with $\text{Cu } K\alpha$ radiation. The resistivity and Hall coefficient were measured using the standard four-probe technique. The heat capacity was measured using the relaxation method. All the transport properties were measured in a Quantum Design physical properties measurement system, PPMS-9. The dc magnetization was obtained using a magnetic property measurement system (Quantum Design, MPMS-VSM).

III. RESULTS AND DISCUSSIONS

Figure 1 shows the XRD pattern of the TlBi_2 sample. Two small peaks marked with asterisks designate the unknown impurity phase, which may come from the oxides. As shown in the figure, most of the peaks can be well indexed with an AlB_2 -type structure (space group $P6/mmm$, No. 191), and

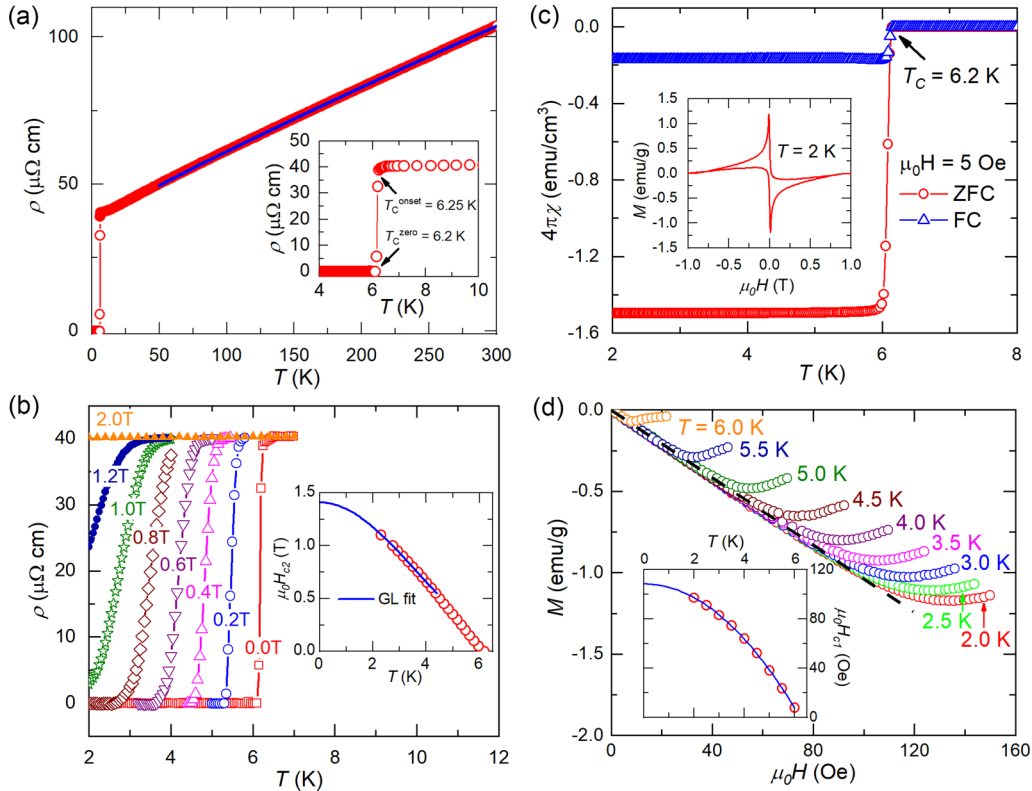


FIG. 2. (a) Temperature dependence of resistivity of TlBi_2 between 2 and 300 K measured at zero field. Inset: enlarged view near T_c . (b) Temperature dependence of resistivity under several selected magnetic fields below 8 K. Inset: upper critical field H_{c2} as a function of temperature for TlBi_2 . (c) Temperature dependence of magnetic susceptibility below 8 K, measured at 5 Oe with both ZFC and FC processes. Inset: Field-dependent magnetization M measured between -1 and 1 T at 2 K. (d) Field-dependent magnetization M measured at various temperatures below 150 Oe. The dashed line indicates the initial linear magnetization curve. Inset: The lower critical field H_{c1} as a function of temperature for TlBi_2 .

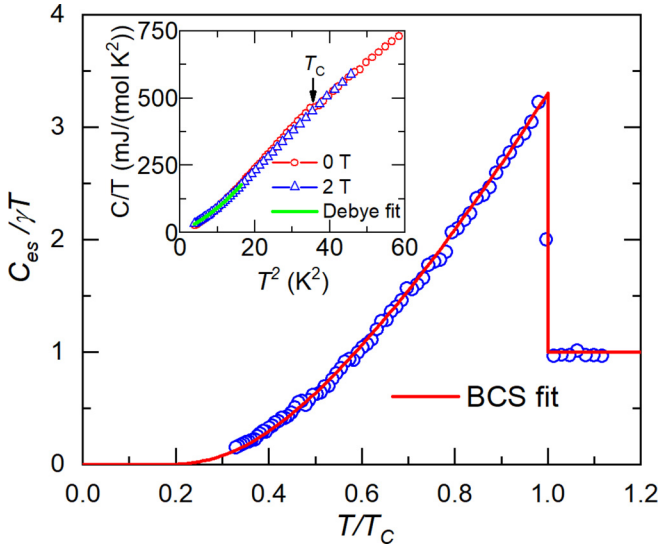


FIG. 3. The electronic specific heat divided by the product of Sommerfeld coefficient γ and temperature as a function of the reduced temperature T/T_c in the superconducting state at zero field. Inset: Temperature square dependence of C/T , measured at 0 and 2 T magnetic fields. The green line is the fit to the data as described in the text.

the lattice parameters $a = 5.6828(2)$ Å, and $c = 3.3731(1)$ Å, were obtained, which is consistent with the results reported previously [12]. The cell parameter a of TlBi₂ is much larger than that of MgB₂ and c is smaller, which originates from the nearly same Bi-Bi bond length along the a and c axes, implying its three-dimensional feature.

Figure 2(a) displays the temperature dependence of the resistivity, $\rho(T)$, between 2 and 300 K of the TlBi₂ sample. The room temperature resistivity $\rho(300$ K) is about 103.7 $\mu\Omega$ cm, close to that of TlSb [16]. It is clear that TlBi₂ exhibits a metallic behavior in the whole measuring temperature range, i.e., the resistivity decreases with decreasing temperature. At $T_{c\text{onset}} = 6.25$ K, the resistivity drops abruptly to zero, suggesting that a bulk superconducting transition occurs with a transition width $\Delta T_c = 0.05$ K, which is also confirmed by a large diamagnetic signal and a significant specific heat jump at T_c , as shown in Figs. 2(c) and Fig. 3, respectively. The superconducting transition temperature here is similar to that reported previously ($T_c = 6.4$ K) [13].

It is obvious that the $\rho(T)$ in the normal state exhibits a linear temperature dependence in a large region (50 K $\leq T \leq 300$ K), which can be ascribed to the low-energy phonon scattering here [17], although the similar behavior in the cuprate high temperature superconductors was explained as the strong electronic correlation effect. As shown by a blue line in Fig. 2(a), we fitted the $\rho(T)$ data above 50 K using the standard Bloch-Grüneisen formula,

$$\rho = \rho_0 + 4C \left(\frac{T}{\Theta_D} \right)^5 \int_0^{T/\Theta_D} \frac{x^5}{(e^x - 1)(1 - e^{-x})} dx, \quad (1)$$

then we obtained the residual resistivity $\rho_0 = 41$ $\mu\Omega$ cm, the fitting parameter $C = 17.5$ $\mu\Omega$ cm/K, and the Debye temperature $\Theta_D = 83$ K. We also found that the $\rho(T)$ below 50 K deviates from the T -linear dependence and turns to T -square

dependence below 20 K, indicating the Fermi-liquid ground state, discussed in detail as follows.

In order to obtain the upper critical field $H_{c2}(T)$, we measured the resistivity at various magnetic fields between 2 and 8 K, as shown in Fig. 2(b). With increasing magnetic field, the superconducting transition shifts to lower temperature. At 2.0 T, the superconducting transition is not observed above 2 K. The H_{c2} is determined by the temperature when the resistivity drops to 50% of the normal-state value and is plotted as a function of temperature in the inset of Fig. 2(b). According to the Ginzburg-Landau (GL) theory, the $\mu_0 H_{c2}$ value at zero temperature was estimated to be 1.4 T using the formula

$$H_{c2}(T) = H_{c2}(0)(1 - t^2)/(1 + t^2), \quad (2)$$

where t is the reduced temperature T/T_c . Then the coherence length ξ_{GL} of TlBi₂ was estimated to be 15.3 nm from the relation, $\xi_{GL}^2 = \Phi_0/2\pi H_{c2}(0)$, where $\Phi_0 = h/2e$ is the magnetic flux quantum ($\approx 2.07 \times 10^{-15}$ Wb).

Figure 2(c) shows the temperature dependence of the magnetic susceptibility, $\chi(T)$, measured at an applied field of 5 Oe both in the zero-field-cooling (ZFC) and field-cooling (FC) processes. A sharp superconducting transition and a quite flat feature below T_c are clearly observed in $\chi(T)$, suggesting superconductivity emerges in the sample. At $T = 2$ K, the $4\pi\chi$ value exceeds -100% emu/cm³ due to the demagnetization effect. The $M(H)$ curve measured at $T = 2$ K, as shown in the inset of Fig. 2(c), exhibits a typical type-II superconducting behavior.

To obtain the lower critical field $H_{c1}(T)$, we measured the $M(H)$ curves at different temperatures, as shown in Fig. 2(d). The $H_{c1}(T)$ determined by the field where M starts to deviate from the initial linear curve, is plotted as a function of temperature in the inset of Fig. 2(d). It is clear that the H_{c1} can be well described using the GL theory as

$$H_{c1}(T) = H_{c1}(0) \left[1 - \left(\frac{T}{T_c} \right)^2 \right]. \quad (3)$$

The lower critical field at zero temperature, $H_{c1}(0)$, was estimated to be 108 Oe. The penetration depth λ_{GL} was estimated to be 198 nm using the relation $H_{c1}(0) = \frac{\Phi_0}{4\pi\lambda_{GL}^2} \ln(\frac{\lambda_{GL}}{\xi_{GL}})$ and the ξ_{GL} value obtained above. Then, the GL parameter, $\kappa_{GL} = \lambda_{GL}/\xi_{GL}$, was calculated to be 12.9, much larger than $1/\sqrt{2}$, confirming that TlBi₂ is a type-II superconductor. The thermodynamic critical field $H_c(0)$ was also estimated to be 770 Oe from the relation $H_{c1}(0)H_{c2}(0) = H_c^2(0)\ln\kappa_{GL}$, which is almost an order of magnitude smaller than that of MgB₂ [2].

To get the information of superconducting transition, we also carried out the specific heat, $C(T)$, measurements at both 0 and 2 T. The inset of Fig. 3 shows the temperature square dependence of C/T with a small difference between the two curves below T_c . The low temperature $C(T)$ measured at 2 T, where bulk superconductivity is completely suppressed, can be well fitted using the Debye model, $C/T = \gamma + \beta T^2 + \delta T^4$, where γ is the Sommerfeld coefficient, β the Debye constant, and δ the fitting parameter. The first and last two terms are ascribed to the electronic and phonon contribution, respectively. We obtained $\gamma = 8.63$ mJ/(mol K²), $\beta = 4.87$ mJ/(mol K⁴), and $\delta = 0.35$ mJ/(mol K⁶) by the best fit to the data below 4 K (the solid green line). Then, the Debye

temperature, Θ_D , was evaluated to be 104 K, which is close to that (83 K) obtained from the $\rho(T)$ data mentioned above, from the relation $\Theta_D = (12\pi^4 RN/5\beta)^{1/3}$, where $R = 8.31$ J/(mol K) is the molar gas constant, and N is the number of atoms per unit cell. The electronic specific heat, $C_{es}(T)$, in the superconducting state was obtained by subtracting the phonon contribution from the total $C(T)$. Figure 3 presents the $C_{es}/\gamma T$ vs T/T_c , a sharp jump of 2.32 emerging at T_c , which is significantly larger than that of the well-known BCS theory (1.43), suggesting that the strong electron-phonon coupling occurs in TlBi₂. The electron-phonon coupling constant, λ_{ep} , can be derived from the modified McMillan formula [18–20]

$$\lambda_{ep} = \frac{1.04 + \mu^* \ln(\frac{\omega_{ln}}{1.2T_c})}{(1 - 0.62\mu^*) \ln(\frac{\omega_{ln}}{1.2T_c}) - 1.04}. \quad (4)$$

where μ^* is the Coulomb pseudopotential, which has been reported to be 0.121 [13], and ω_{ln} is the logarithmic averaged phonon frequency, which can be estimated from the specific heat jump at T_c using the formula [18–20]

$$\frac{\Delta C}{\gamma T_c} = 1.43 \times \left[1 + 53 \left(\frac{T_c}{\omega_{ln}} \right)^2 \ln \left(\frac{\omega_{ln}}{3T_c} \right) \right]. \quad (5)$$

Taking $\Delta C/\gamma T_c = 2.32$ and $T_c = 6.2$ K, we obtained $\omega_{ln} = 63.3$ K and $\lambda_{ep} = 1.38$, which is smaller than $\lambda_{ep} = 1.63$ reported previously [13]. However, it is still large compared with those for typical strong-coupling superconductors such as Mo₆Se₈ ($\lambda_{ep} = 1.27$), and Pb-Tl alloy ($\lambda_{ep} = 1.15$ – 1.53) [18], indicating the strong-coupling nature of superconducting pairing.

Then, we analyzed the electronic specific heat data $C_{es}(T)$ using BCS theory with a single gap. Within the framework of BCS theory, the thermodynamic properties, entropy (S) and electronic specific heat (C_{es}), can be written as

$$S = -\frac{6\gamma}{\pi^2} \frac{\Delta_0}{k_B} \int_0^\infty [f \ln f + (1-f) \ln(1-f)] dy, \quad (6)$$

$$C_{es} = T \frac{dS}{dT}, \quad (7)$$

where $f = [\exp(\beta E) + 1]^{-1}$ and $\beta = (k_B T)^{-1}$, whereas the integration variable is $y = \varepsilon/\Delta_0$. The energy of the quasiparticles is evaluated from the relation $E = [\varepsilon^2 + \Delta_0^2 \delta^2(t)]^{0.5}$, where ε is electron energy with respect to the Fermi energy and $\delta(t)$ is the normalized BCS gap at the reduced temperature $t = T/T_c$ as tabulated by Mühlischlegel [21]. As shown in the figure, the single-gap model presents a good fit to $C_{es}/\gamma T$, suggesting that TlBi₂ is a phonon-mediated s -wave superconductor. Meanwhile, the $\Delta_0/k_B T_c$ that was fitted to be 2.25, agrees well with that obtained from the tunneling experiments [22], which is much larger than that as predicted for a weak-coupling limit ($\Delta_0/k_B T_c = 1.76$), further confirming the strong electron-phonon coupling in TlBi₂. The obtained superconducting parameters are summarized in Table I.

Figure 4 shows the temperature dependence of the Hall coefficient R_H of TlBi₂. The transverse Hall resistivity, ρ_{yx} , was derived from the antisymmetric part of the transverse resistivity under the reversal of magnetic field at a given temperature. As shown in the inset of Fig. 4, the ρ_{yx} exhibits a linear dependence with the magnetic field below 9 T, suggesting that R_H is independent of the magnetic field. At

TABLE I. The superconducting parameters for TlBi₂ superconductor.

Parameters (unit)	Value
T_c (K)	6.2
$\mu_0 H_{c1}(0)$ (T)	1.08×10^{-2}
$\mu_0 H_{c2}(0)$ (T)	1.4
ξ_{GL} (nm)	15.3
λ_{GL} (nm)	198
κ_{GL}	12.9
λ_{ep}	1.38
γ (mJ/mol K ²)	8.63
$\Delta C_{es}/\gamma T_c$	2.32
$\Delta_0/k_B T_c$	2.25

$T = 10$ K, R_H is about -1.9×10^{10} m³/C, indicating that the dominant carriers are electron type. With increasing temperature, R_H increases monotonically, but remains negative below 300 K. The significant T -dependent behavior of R_H is similar to that observed in MgB₂ [23]. If we assume that the Drude relation holds for TlBi₂ even in the case of multiple bands, the carrier concentration n could be estimated to be 3.3×10^{22} /cm³ at $T = 10$ K. Assuming a parabolic dispersion with spherical Fermi surface, the Fermi wave vector, k_F , could be calculated to be 9.9×10^9 m⁻¹ from $k_F = (3n\pi^2)^{1/3}$. Then the band Sommerfeld coefficient γ_b was calculated to be 3.0 mJ/(mol K²) from the relation $\gamma_b = \pi^2 n k_B^2 m_e / \hbar^2 k_F^2$. In a strong-coupling compound, the electronic specific heat coefficient γ_{cal} is expected to enhance to be $(1 + \lambda_{ep})\gamma_b$ due to electron-phonon coupling [17,24], where λ_{ep} is the electron-phonon coupling constant. Using the value for λ_{ep} (1.38) determined from our measurements, the γ_{cal} is calculated to be 7.14 mJ/(mol K²), which is close to that obtained from the specific heat measurements, indicating that the Fermi-liquid theory can well describe the behavior of the TlBi₂ compound.

The KWR compares the temperature dependence of a metal's resistivity to that of its specific heat [35,37], thereby probing the relationship between the electron-electron scattering rate and the renormalization of the electron mass,

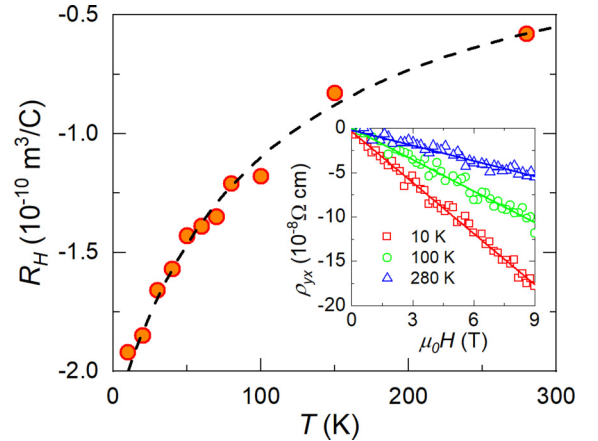


FIG. 4. Temperature dependence of the Hall coefficient R_H of TlBi₂ between 10 and 280 K. The dashed line is a guide for eyes. Inset: Isothermal Hall resistivity at $T = 10$, 100, and 280 K.

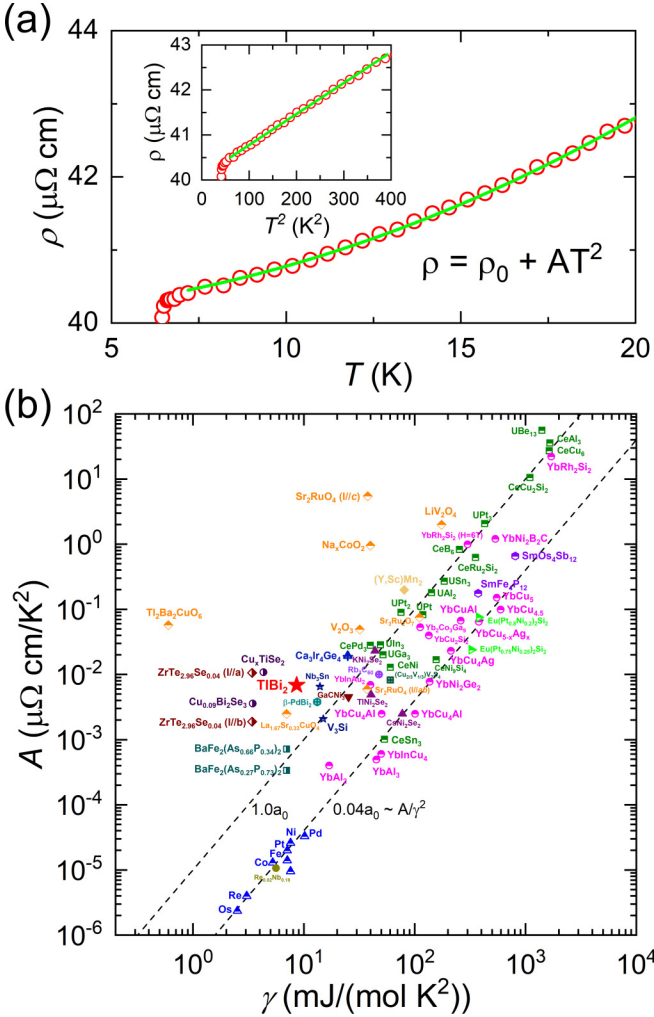


FIG. 5. (a) Temperature dependence of resistivity below 20 K. Inset: temperature square dependence of resistivity below 20 K. The solid green lines correspond to $\rho = \rho_0 + AT^2$, just as mentioned in the main text. (b) The coefficient A vs the Sommerfeld coefficient γ for various compounds. The data beyond TlBi_2 were collected from previous papers [25], including CDW materials [26,27], oxides [28–33], A-15 superconductors [34], heavy fermions [33,35,36], transition metals [37], and so on [38,39].

which is considered as a measurement of the electron-electron correlation strength. In other words, the KWR in heavy fermion compounds is larger than that in transition metals due to the stronger correlation [34]. Furthermore, the KWR value for many heavy-fermion compounds is close to $1.0 \times 10^{-5} \mu\Omega \text{ cm}(\text{mol K}^2/\text{mJ})^2 = 1.0a_0$, while for a lot of transition metals, the KWR value is close to $0.04 \times 10^{-5} \mu\Omega \text{ cm}(\text{mol K}^2/\text{mJ})^2 = 0.04a_0$ [32,35], where $a_0 = 10^{-5} \mu\Omega \text{ cm}(\text{mol K}^2/\text{mJ})^2$. To deduce the KWR value of TlBi_2 , we fitted the $\rho(T)$ data between 7 and 20 K using the Fermi-liquid prediction, $\rho = \rho_0 + AT^2$, when electron-electron scattering dominates over electron-phonon scattering. The residual resistivity $\rho_0 = 40.1 \mu\Omega \text{ cm}$ and the coefficient $A = 6.84 \times 10^{-3} \mu\Omega \text{ cm/K}^2$ were obtained by the fitting, as shown in Fig. 5(a). Using the Sommerfeld coefficient $\gamma = 8.63 \text{ mJ}/(\text{mol K}^2)$ obtained from $C(T)$

measurement, we obtained the KWR of TlBi_2 to be $9.2 \times 10^{-5} \mu\Omega \text{ cm}(\text{mol K}^2/\text{mJ})^2$. For comparison, we plot the KWR of various compounds in Fig. 5(b). It is obvious that the KWR value of TlBi_2 obtained here is somehow very large.

To explain the unexpectedly large KWR in other compounds, several scenarios have been proposed. For example, Miyake *et al.* suggested that the large KWR of UBe_{13} may be ascribed to its f electrons and large residual resistivity [34]. Li *et al.* proposed that a possible mechanism of the large KWR is in proximity to a quantum critical point in $\text{Na}_{0.7}\text{Co}_2\text{O}_2$ [29]. Strack *et al.* also suggested that the electron-phonon scattering in reduced dimensions may result in a quadratic temperature-dependent resistivity, which may lead to the large KWR of $\kappa\text{-(BEDT-TTF)}_2\text{Cu[N(CN)}_2\text{]Br}$ [40]. Specifically, Matsuura *et al.* [41,42] suggested that the strong dynamical coupling between conduction electrons and phonons may give rise to the heavy fermion bands at low temperatures. Thus, the strong-coupling compounds, such as Nb_3Sn and V_3Si [34], may obey the universal KWR of heavy fermion compounds, i.e., $A/\gamma^2 \approx 10^{-5} \mu\Omega \text{ cm}(\text{mol K}^2/\text{mJ})^2$. In the TlBi_2 case, the electronic correlation seems not so strong as discussed above. Considering the characteristics of strong coupling, we suggest that the mechanism of the large KWR in TlBi_2 may be similar to that in Nb_3Sn and V_3Si . However, it is worth noting that our KWR value is almost an order of magnitude larger than that obtained in V_3Si and many heavy fermion compounds, suggesting that other mechanisms also need to be considered. From this point of view, TlBi_2 may provide a novel material platform for studying large KWR and its relationship with superconductivity.

IV. CONCLUSION

In summary, we systematically investigated the superconducting and normal-state properties of TlBi_2 . Type-II superconductivity with $T_c = 6.2 \text{ K}$, the upper critical field $\mu_0 H_{c2} = 1.4 \text{ T}$, and the lower critical field $\mu_0 H_{c1} = 1.08 \times 10^{-2} \text{ T}$ was revealed by the resistivity and magnetization measurements. It was found that the electronic specific heat in the superconducting state can be well described using a single-gap model within the BCS framework. The strong electron-phonon coupling occurs in this compound, confirmed by both the large λ_{ep} (1.38) and the large $\Delta_0/k_B T_c$ (2.25) values, indicating that TlBi_2 is a conventional superconductor. In the normal state, the resistivity exhibits T -linear dependence above 50 K, which is ascribed to the low-energy phonon scattering, and T -square dependence below 20 K, suggesting the Fermi-liquid ground state. Combining the specific heat data at normal state, a large KWR [$9.2 \times 10^{-5} \mu\Omega \text{ cm}(\text{mol K}^2/\text{mJ})^2$] was obtained, which is an order of magnitude larger than that obtained in many heavy fermion compounds, although the electronic correlation is not so strong.

ACKNOWLEDGMENTS

This work was supported by the Ministry of Science and Technology of China under Grant No. 2022YFA1403202, the National Natural Science Foundation of China (NSFC) under Grants No. 11974095 and No. 12074335, and the Fundamental Research Funds for the Central Universities.

- [1] J. Nagamatsu, N. Nakagawa, T. Muranaka, Y. Zenitani, and J. Akimitsu, Superconductivity at 39 K in magnesium diboride, *Nature (London)* **410**, 63 (2001).
- [2] X. Xi, Two-band superconductor magnesium diboride, *Rep. Prog. Phys.* **71**, 116501 (2008).
- [3] K.-P. Bohnen, R. Heid, and B. Renker, Phonon Dispersion and Electron-Phonon Coupling in MgB_2 and AlB_2 , *Phys. Rev. Lett.* **86**, 5771 (2001).
- [4] T. Yildirim, O. Gülseren, J. W. Lynn, C. M. Brown, T. J. Udovic, Q. Huang, N. Rogado, K. A. Regan, M. A. Hayward, J. S. Slusky, T. He, M. K. Haas, P. Khalifah, K. Inumaru, and R. J. Cava, Giant Anharmonicity and Nonlinear Electron-Phonon Coupling in MgB_2 : A Combined First-Principles Calculation and Neutron Scattering Study, *Phys. Rev. Lett.* **87**, 037001 (2001).
- [5] J. M. An and W. E. Pickett, Superconductivity of MgB_2 : Covalent Bonds Driven Metallic, *Phys. Rev. Lett.* **86**, 4366 (2001).
- [6] J. Kortus, I. I. Mazin, K. D. Belashchenko, V. P. Antropov, and L. L. Boyer, Superconductivity of Metallic Boron in MgB_2 , *Phys. Rev. Lett.* **86**, 4656 (2001).
- [7] I. I. Mazin, O. K. Andersen, O. Jepsen, O. V. Dolgov, J. Kortus, A. A. Golubov, A. B. Kuz'menko, and D. van der Marel, Superconductivity in MgB_2 : Clean or Dirty?, *Phys. Rev. Lett.* **89**, 107002 (2002).
- [8] H. J. Choi, D. Roundy, H. Sun, M. L. Cohen, and S. G. Louie, The origin of the anomalous superconducting properties of MgB_2 , *Nature (London)* **418**, 758 (2002).
- [9] M. Iavarone, G. Karapetrov, A. E. Koshelev, W. K. Kwok, G. W. Crabtree, D. G. Hinks, W. N. Kang, E.-M. Choi, H. J. Kim, H.-J. Kim, and S. I. Lee, Two-band Superconductivity in MgB_2 , *Phys. Rev. Lett.* **89**, 187002 (2002).
- [10] K.-H. Jin, H. Huang, J.-W. Mei, Z. Liu, L.-K. Lim, and F. Liu, Topological superconducting phase in high- T_c superconductor MgB_2 with Dirac-nodal-line fermions, *npj Comput. Mater.* **5**, 57 (2019).
- [11] X. Zhou, K. N. Gordon, K.-H. Jin, H. Li, D. Narayan, H. Zhao, H. Zheng, H. Huang, G. Cao, N. D. Zhigadlo, F. Liu, and D. S. Dessau, Observation of topological surface states in the high-temperature superconductor MgB_2 , *Phys. Rev. B* **100**, 184511 (2019).
- [12] E. Makarkov, Crystal structure of the gamma phase of the systems Al-Mg and Ti-Bi, *Dokl. Akad. Nauk SSSR* **74**, 935 (1950).
- [13] R. Dynes, McMillan's equation and the T_c of superconductors, *Solid State Commun.* **10**, 615 (1972).
- [14] T. Claeson and O. Östklint, Phase transformation and electron structure effects in Bi-Tl, *Acta Metall.* **22**, 759 (1974).
- [15] F. Izumi and T. Ikeda, A Rietveld-analysis program RIETAN-98 and its applications to zeolites, in *Materials Science Forum* (Trans Tech Publ, 2000), Vol. 321, pp. 198–205.
- [16] Y. Zhou, B. Li, Z. Lou, H. Chen, Q. Chen, B. Xu, C. Wu, J. Du, J. Yang, H. Wang, and M. Fang, Bulk superconductivity in the Dirac semimetal TiSb , *Sci. China Phys. Mech. Astron.* **64**, 1 (2021).
- [17] T. Takayama, K. Kuwano, D. Hirai, Y. Katsura, A. Yamamoto, and H. Takagi, Strong Coupling Superconductivity at 8.4 K in an Antiperovskite Phosphide SrPt_3P , *Phys. Rev. Lett.* **108**, 237001 (2012).
- [18] P. B. Allen and R. C. Dynes, Transition temperature of strong-coupled superconductors reanalyzed, *Phys. Rev. B* **12**, 905 (1975).
- [19] J. P. Carbotte, Properties of boson-exchange superconductors, *Rev. Mod. Phys.* **62**, 1027 (1990).
- [20] T. Klimczuk, F. Ronning, V. Sidorov, R. J. Cava, and J. D. Thompson, Physical Properties of the Noncentrosymmetric Superconductor $\text{Mg}_{10}\text{Ir}_{19}\text{B}_{16}$, *Phys. Rev. Lett.* **99**, 257004 (2007).
- [21] B. Mühlischlegel, Die thermodynamischen funktionen des supraleiters, *Z. Phys.* **155**, 313 (1959).
- [22] P. Vashishta and J. P. Carbotte, Some Finite-Temperature Properties of Superconducting Bi_2Ti , *Phys. Rev. B* **10**, 2789 (1974).
- [23] R. Jin, M. Paranthaman, H. Y. Zhai, H. M. Christen, D. K. Christen, and D. Mandrus, Unusual Hall effect in superconducting MgB_2 films, *Phys. Rev. B* **64**, 220506(R) (2001).
- [24] M. Brühwiler, S. M. Kazakov, J. Karpinski, and B. Batlogg, Mass enhancement, correlations, and strong-coupling superconductivity in the β -pyrochlore KOs_2O_6 , *Phys. Rev. B* **73**, 094518 (2006).
- [25] Y. Fang, W.-L. You, and M. Li, Unconventional superconductivity in $\text{Cu}_x\text{Bi}_2\text{Se}_3$ from magnetic susceptibility and electrical transport, *New J. Phys.* **22**, 053026 (2020).
- [26] K. E. Wagner, E. Morosan, Y. S. Hor, J. Tao, Y. Zhu, T. Sanders, T. M. McQueen, H. W. Zandbergen, A. J. Williams, D. V. West, and R. J. Cava, Tuning the charge density wave and superconductivity in Cu_xTaS_2 , *Phys. Rev. B* **78**, 104520 (2008).
- [27] X. Zhu, W. Ning, L. Li, L. Ling, R. Zhang, J. Zhang, K. Wang, Y. Liu, L. Pi, Y. Ma, H. Du, M. Tian, Y. Sun, C. Petrovic, and Y. Zhang, Superconductivity and charge density wave in $\text{ZrTe}_{3-x}\text{Se}_x$, *Sci. Rep.* **6**, 1 (2016).
- [28] Y. Maeno, K. Yoshida, H. Hashimoto, S. Nishizaki, S.-i. Ikeda, M. Nohara, T. Fujita, A. P. Mackenzie, N. E. Hussey, J. G. Bednorz, and F. Lichtenberg, Two-dimensional Fermi liquid behavior of the superconductor Sr_2RuO_4 , *J. Phys. Soc. Jpn.* **66**, 1405 (1997).
- [29] S. Y. Li, L. Taillefer, D. G. Hawthorn, M. A. Tanatar, J. Paglione, M. Sutherland, R. W. Hill, C. H. Wang, and X. H. Chen, Giant Electron-Electron Scattering in the Fermi-Liquid State of $\text{Na}_{0.7}\text{CoO}_2$, *Phys. Rev. Lett.* **93**, 056401 (2004).
- [30] C. Urano, M. Nohara, S. Kondo, F. Sakai, H. Takagi, T. Shiraki, and T. Okubo, LiV_2O_4 Spinel as a Heavy-Mass Fermi Liquid: Anomalous Transport and Role of Geometrical Frustration, *Phys. Rev. Lett.* **85**, 1052 (2000).
- [31] S. Nakamae, K. Behnia, N. Mangkorntong, M. Nohara, H. Takagi, S. J. C. Yates, and N. E. Hussey, Electronic ground state of heavily overdoped nonsuperconducting $\text{La}_{2-x}\text{Sr}_x\text{CuO}_4$, *Phys. Rev. B* **68**, 100502(R) (2003).
- [32] A. Jacko, J. Fjærestad, and B. Powell, A unified explanation of the Kadowaki-Woods ratio in strongly correlated metals, *Nat. Phys.* **5**, 422 (2009).
- [33] N. Tsujii, K. Yoshimura, and K. Kosuge, Deviation from the Kadowaki-Woods relation in Yb-based intermediate-valence Systems, *J. Phys.: Condens. Matter* **15**, 1993 (2003).
- [34] K. Miyake, T. Matsuura, and C. Varma, Relation between resistivity and effective mass in heavy-fermion and A15 compounds, *Solid State Commun.* **71**, 1149 (1989).
- [35] K. Kadowaki and S. Woods, Universal relationship of the resistivity and specific heat in heavy-fermion compounds, *Solid State Commun.* **58**, 507 (1986).

- [36] N. Tsujii, H. Kontani, and K. Yoshimura, Universality in Heavy Fermion Systems with General Degeneracy, *Phys. Rev. Lett.* **94**, 057201 (2005).
- [37] M. J. Rice, Electron-Electron Scattering in Transition Metals, *Phys. Rev. Lett.* **20**, 1439 (1968).
- [38] H. Wang, C. Dong, Q. Mao, R. Khan, X. Zhou, C. Li, B. Chen, J. Yang, Q. Su, and M. Fang, Multiband Superconductivity of Heavy Electrons in a TiNi_2Se_2 Single Crystal, *Phys. Rev. Lett.* **111**, 207001 (2013).
- [39] J. Huimin Chen, J. Yang, C. Cao, L. Li, Q. Su, B. Chen, H. Wang, Q. Mao, B. Xu, J. Du, and M. Fang, Superconductivity in a new layered nickel selenide CsNi_2Se_2 , *Supercond. Sci. Technol.* **29**, 045008 (2016).
- [40] C. Strack, C. Akinci, V. Paschenko, B. Wolf, E. Uhrig, W. Assmus, M. Lang, J. Schreuer, L. Wiehl, J. A. Schlueter, J. Wosnitzer, D. Schweitzer, J. Müller, and J. Wykhoff, Resistivity studies under hydrostatic pressure on a low-resistance variant of the quasi-two-dimensional organic superconductor $\kappa\text{-(BEDT-TTF)}_2\text{Cu[N(CN)}_2\text{]Br}$: Search for intrinsic scattering contributions, *Phys. Rev. B* **72**, 054511 (2005).
- [41] T. Matsuura and K. Miyake, Heavy fermion aspects of strong electron-phonon coupling compound, *J. Phys. Soc. Jpn.* **55**, 610 (1986).
- [42] C. C. Yu and P. W. Anderson, Local-phonon model of strong electron-phonon interactions in A15 compounds and other strong-coupling superconductors, *Phys. Rev. B* **29**, 6165 (1984).